Available online at www.sciencedirect.com

SciVerse ScienceDirect

Ceramics International 39 (2013) 6695–6702

CERAMICS INTERNATIONAL

www.elsevier.com/locate/ceramint

Microstructure and mechanical properties of fine grained carbon-bonded Al_2O_3–C materials

Y. Klemm[a,*], H. Biermann[a], C.G. Aneziris[b]

[a]Technische Universität Bergakademie Freiberg, Institute of Materials Engineering, Gustav-Zeuner-Straße 5, 09599 Freiberg, Germany
[b]Technische Universität Bergakademie Freiberg, Institute of Ceramic, Glass and Construction Materials, Agricolastraße 17, 09599 Freiberg, Germany

Received 28 November 2012; received in revised form 9 January 2013; accepted 16 January 2013
Available online 7 February 2013

Abstract

Fine grained carbon-bonded Al_2O_3–C materials as used in ceramic filters have been manufactured by uniaxial and isostatic pressing, respectively. The variation in the microstructure over the cross section of the samples which in particular depends on the shaping technique plays an important role in the wetting of the material by liquid steel. Moreover, the amount and grain size of the binder has a decisive influence on the porosity and bulk density and therefore on the mechanical properties. For this, two different grain size distributions of Carbores® P binder were used, and in addition the fraction of binder was varied from 5–30 wt%. Tests of the cold crushing strength and of the cold modulus of rupture were performed at room temperature. The adjusted bulk density, open porosity and shrinkage of the samples were determined and the microstructure was analyzed by means of scanning electron microscopy. For control of a homogeneous distribution of carbon in the samples, the residual carbon content was measured also within individual samples at different positions.

Keywords: D. Al_2O_3; D. Carbon; E. Refractories; Ceramic bulk material; Mechanical strength

1. Introduction

For the production of clean high quality cast steel components ceramic filters are applied in the last decade in order to reduce non-metallic inclusions [1]. The filter materials have to fulfill different thermo mechanical requirements and especially to withstand the thermal shock attack in the beginning of the steel melt casting [2,4]. Carbon-bonded alumina materials provide an excellent thermo mechanical performance and are since several years used in functional components such as submerged entry nozzles, stoppers etc., whereby coarse grain size distributions up to 1 mm are used [3]. In carbon bonded filter materials due to the small strut thickness in the area of 300–400 μm only fine grains up to 30–40 μm are acceptable [6]. Therefore the main approach of this contribution is the manufacturing of bulk samples due to pressing with approximately the same pore size and grain size distribution in order to be able to characterize the mechanical properties of the fine grained Al_2O_3–C materials as used in filter applications. These mechanical properties will be used for the simulation of the filter behavior and the development of constitutive laws.

As binder as well as a carbon source Carbonaceous Resin (Rütgers Chemicals AG, Germany) with a lower amount of carcinogenic polycyclic aromatic hydrocarbons (300 ppm) than standard pitch (10.000 ppm) is used. The high residual graphitic like carbon amount derived from the Carbores® P binder has compared to phenolic resins the advantage of higher flexibility and high thermal conductivity combined with low Coefficient of Thermal Expansion (CTE) which result in an excellent thermal shock and oxidation resistance [5,7].

2. Materials and methods

2.1. Raw materials and processing

In Table 1 the compositions of the specimens used for the production of bulk carbon-bonded Al_2O_3–C are listed.

*Corresponding author. Tel.: +49 37 3139 3727.
E-mail address: Yvonne.Klemm@iwt.tu-freiberg.de (Y. Klemm).

0272-8842/$ - see front matter © 2013 Elsevier Ltd and Techna Group S.r.l. All rights reserved.
http://dx.doi.org/10.1016/j.ceramint.2013.01.108

Table 1
Composition of the investigated samples [wt%].

	AC 5	AC 10	AC 15	AC 20	AC 30
Al_2O_3 martoxid® MR70	66	66	66	66	66
Carbores® P	5	10	15	20	30
Carbon black MT N–991	13	11	9	6	2
Grafite AF 96/97	16	13	10	8	2

Table 2
Particle size distribution of the raw materials [μm].

	d10	d50	d90
Al_2O_3 martoxid® MR70	0.2–0.4	0.5–0.8	1.5–3
Carbores® P coarse‘	–	80	400
Carbores® P fine‘	1.8	4.9	11.6
Carbon black MT N–991	0.2	1.1	9.3
Grafite AF 96/97	≤4	8.5–11	≤25

The materials have a content of 66 wt% fine alumina Martoxid® MR70 from Albemarle (Bergheim, Germany). As binder Carbores® P (CARBO naceous RESin) from Rütgers Chemicals (Castrop-Rauxel, Germany), which is a high melting coal-tar resin, with two different particle size distributions (cf. Table 2) was applied with contents of 5 to 30 wt%. Carbores® P softens at temperatures higher than 200 °C and has a highly oriented graphite-like carbon structure after coking [2]. The coke residue of Carbores® P is up to 85%.

Furthermore carbon black MT-Thermax N991 from Lehmann & Voss (Hamburg, Germany) and graphite AF 96/97 of Graphit Kropfmühl (Kropfmühl, Germany) were used with different fractions.

The raw materials were dry mixed in an Eirich mixer for about 5 min. Afterwards, granules were produced with the addition of water and 1% Glycerol. The formation of the granules depended on the fraction of the binder in the mixture. As the moisture content was too high for compression, the granules were afterwards dried in a drying oven at 60 °C down to a moisture content below 3%. Afterwards, shaping by uniaxial and isostatic pressing has been performed, respectively. Cylinders (diameter: 50 mm, height: 50 mm) and bending bars (7 mm × 7 mm × 70 mm) were pressed at 150 MPa at a lab press ES 270.00 of Rucks Maschinenbau GmbH, Germany.

The isostatic pressing was also carried out at a pressure of 150 MPa at a SO 5-8359-0 of EPSI NV., Belgium, with a holding time of 1 min at the maximal pressure. In order to avoid skin effects samples of 50 mm × 50 mm and 7 mm × 7 mm × 70 mm were cut out.

After shaping, the green samples were coked up to 800 °C at a heating rate of 1 K/min and a holding time of 30 min after each 100 °C step and of 3 h at 800 °C according to conventional filter materials, Fig. 1. The samples are embedded in a retort filled with calcined petcoke (Müco, Germany) and heated in a Nabertherm (Germany) LH 15/14 furnace. This leads to the formation of a coke network, the binding matrix, into which the alumina particles are integrated.

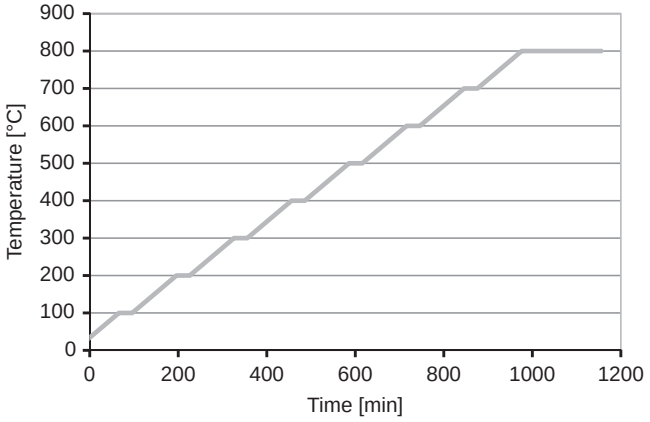

Fig. 1. Heating curve for thermal treatment.

2.2. Experimental techniques

The bulk density, the open porosity and pore size distribution were measured using a Pascal mercury porosimeter (Pascal 440, Thermo Fisher Scientific, Germany). To obtain the shrinkage, the width and length of the sample were measured before and after pyrolysis.

Due to changes in raw material contents, this may influence the quantitative amount of carbon in total and its distribution in the sample. As this will influence the mechanical properties, it is important to determine the residual carbon content. About 20 mg of material was fired under an oxidizing atmosphere in a carbon analyzer (RC 412, Leco, USA) under formation of CO_2. The firing curve from 20 °C to 1000 °C was measured with a heating rate of 62 K/min. The carbon measurement results from changes in mass of the sample. For an investigation of the distribution of carbon in the sample, material from the top surface and from the center area, respectively, was subject to the oxidation test, Fig. 2.

The microstructure of the materials was studied with a field emission scanning electron microscope (MIRA3, TESCAN, Brno, Czech Republic). Specimens were prepared by cutting and mechanical polishing with a final diamond grade of 1 μm.

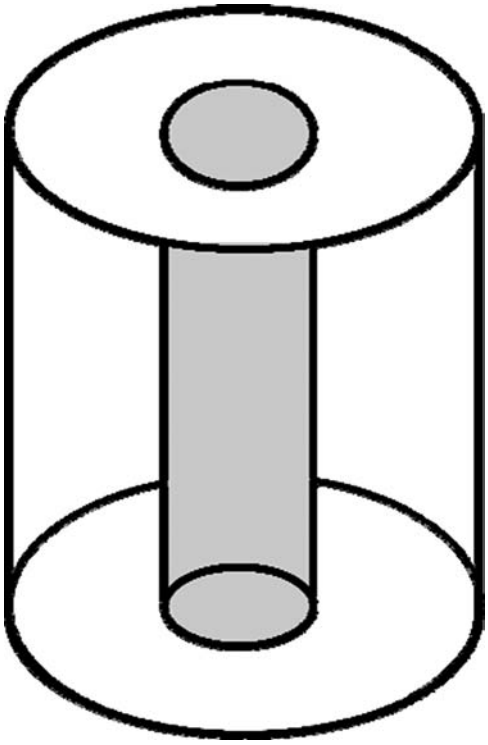

Fig. 2. Places of sampling for measuring carbon content distribution in the sample.

3-point-bending tests were performed on a universal testing machine (TT 2420, TIRA GmbH, Germany) with a load sensor of 1 kN. The displacement speed was 1.5 mm/min until a force of 3 N was reached. At this point, the displacement speed was increased to 2 mm/min. The end of the experiment was set when a strength loss of 50% was reached. A minimum of 10 samples were tested, to obtain the cold modulus of rupture (CMOR).

The cold crushing strength (CCS) was also measured on a universal testing machine (TT 2420, TIRA GmbH, Germany) with a load sensor of 20 kN and a minimum of 10 bending bars. The displacement speed was 5 mm/min up to a force of 20 N. The test was ongoing with a speed of 1 $N/mm^2/s$. The test was stopped at a strength loss of 50%.

The strength of the granules was measured with an AccuPyc 1330 V2.01 testing device (Dr. Axel Hesse Werkstoff- & Prüftechnik Keramik, Germany). It consists of three components:

- a table housing including the motor control and power supply,
- a force signal converter and
- the test apparatus (Fig. 3).

First the sample must be placed on the support. After that the estimated diameter of the granule is required. The plunger is now moved up to the sample. When the force is more than 0.002 N, measuring starts. The test has to be finished manually if the fracture is visible and the load-displacement curve declines.

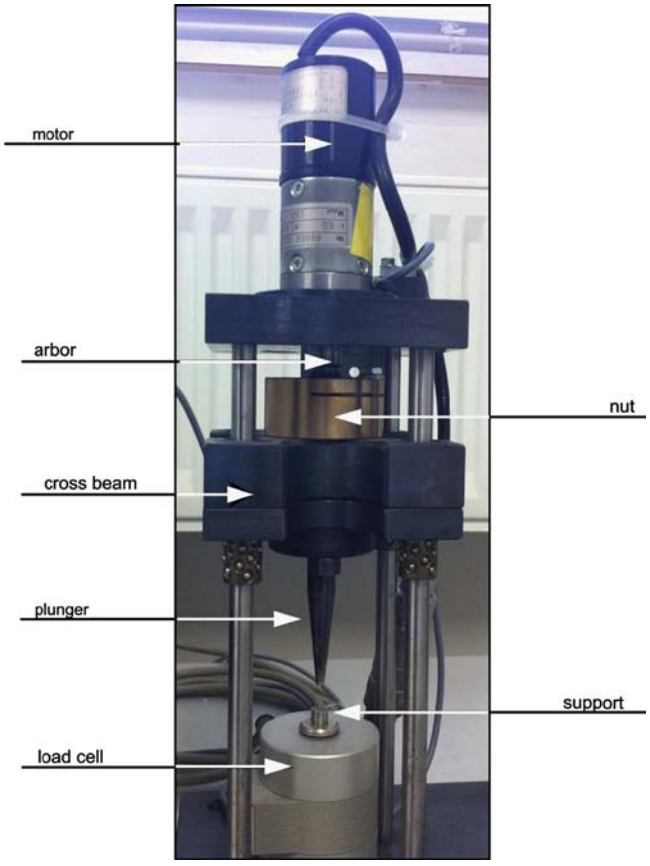

Fig. 3. Testing machine.

3. Results

The resulting microstructure of the carbon bonded Al_2O_3–C is emerged through shaping and coking. At uniaxial pressing the material is compressed single-sided whereas density should be higher on the bottom of the sample than on the top. Additionally, a varying density distribution is also caused through the wall friction between plunger and mold. These effects in turn affect the local properties [8], In addition, an orientation of the graphite flakes perpendicular to the pressing direction developed which increases the anisotropy of the green uniaxially pressed samples. In isostatic pressing the pressure is all sided on the latex mold which gives a uniform density distribution.

During coking the anisotropy of the structure is generated by the formation of liquid crystal phases [9]. Volatile constituents are transported to the surface and released. Isostatically pressed samples burst completely during pyrolysis especially if the binder content was larger than 20 wt%. Samples with a lower binder amount generated macro cracks on the surface and were not acceptable for further investigations. The shaping of samples through uniaxial pressing at 150 MPa produces macro crack free samples.

Observing a fracture surface after the bending strength test of the uniaxially pressed samples the original granules

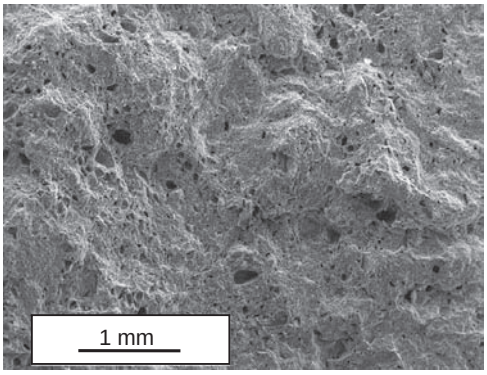

Fig. 4. SEM image of fracture surface of a bending stick with 15 wt% Carbores.

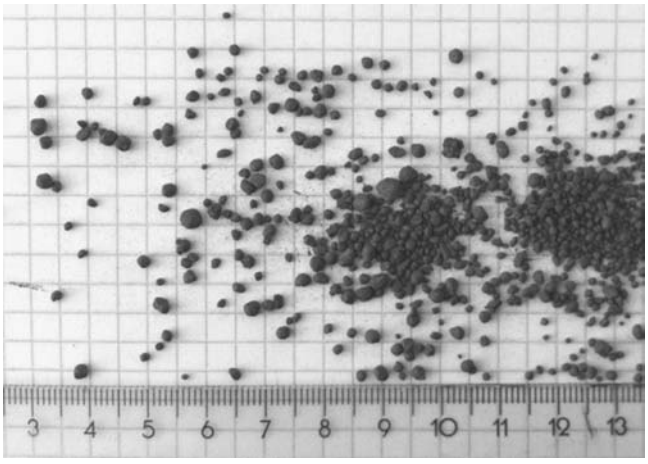

Fig. 5. Al_2O_3–C granules.

were still visible, Fig. 4. Because of their strength they could not be destroyed at all during pressing, which led to lower densities and early fracture of the specimen since the crack was running between the granules.

According to Fig. 5 the size of the produced granules ranges from 5 mm to 1 mm. Apart from that, the granulate contains also fines. According to Schulle the ratio of coarse and fine granules (>0.5 mm and <0.125 mm) should be lower than 5% [11]. That means the granules in Fig. 5 are oversized. Producing granules in the range of 0.5 mm to 0.125 mm depends on the granulating process.

The main class of the granules with more than 50% was lying in the range of 1 to 1.6 mm. Exemplarily the distribution of the strength of a fraction of ten granules in the range of 1 to 1.6 mm is listed in Table 3. The strength was measured according to the standard compression strength $\sigma = 4 \times F/\pi \times d^2$ without consideration of the deformation. In Table 3 there are 10 measured values ranging from 0.03 MPa up to 0.65 MPa with a standard deviation of 0.24 MPa. However, no clear dependency of the strength values from the granule diameters was obtained. Whereas the distribution of the compression strength of the granules is independent on the diameter,

Table 3
Strength of granules with 15 wt% Carbores: *d*—diameter of the granule, *S*—absolute deformation in the direction of compression, *F*—load at failure, σ—granule strength as ball compression strength.

No	d [mm]	S [mm]	F [N]	σ [MPa]
1	1.31	0.05	0.74	0.55
2	1.58	0.02	0.06	0.03
3	1.73	0.02	0.64	0.27
4	1.04	0.03	0.12	0.14
5	1.60	0.02	0.05	0.03
6	1.48	0.08	0.81	0.47
7	1.99	0.04	0.27	0.08
8	2.14	0.01	0.44	0.12
9	1.16	0.04	0.69	0.65
10	1.42	0.20	0.86	0.54

the residual moisture may have a significant influence on the strength and its distribution. The moisture of the granulate material reached an average value of 1.54%. The allocation of moisture in the granules may alternate and causes different strengths what mainly influences the pressing process.

Lucke found on granules of porcelain mass particularly that residual moisture contents of 0% and 3.5% provide highest crushing strengths. Due to this fact, in case of pressing, few interfaces were formed which results in lower preform strength. A moisture content of 2% leads to lowest strengths of granules. This is in turn optimum for pressing because the granules can deform even at low stresses and many interfaces between the granules can form. Thus, the preform has a uniform structure and good strength [10]. Schulle reported that the most important point for pressing is to keep the residual moisture lower than 3%. Instead it happens that the granules clog and insufficient dearing occurs. Because of inadequate green fracture strength the residual moisture should be above 1% [11].

3.1. Cold modulus of rupture

The Carbores content has a significant effect on the bending strength, Fig. 6. It becomes apparent that the CMOR increases with higher binder contents and the 30 wt% binder content offers the highest CMOR of 18 MPa. The samples containing 15 wt% fine Carbores showed an average CMOR of 19 MPa. Compared to this, the samples with 15 wt% coarse Carbores binder exhibit a CMOR of 11 MPa. In both cases of fine and coarse Carbores the granules were not destroyed. It is assumed that a microstructure without the detrimental effect of the granules should have significantly higher CMOR values.

3.2. Cold crushing strength

The value of CCS shown in Fig. 7 increased from 15 MPa for 5 wt% binder content up to 44 MPa for 20 wt% Carbores

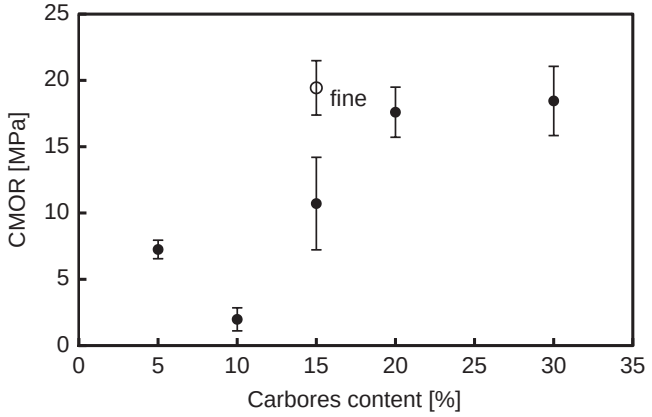

Fig. 6. Cold modulus of rupture at different Carbores contents.

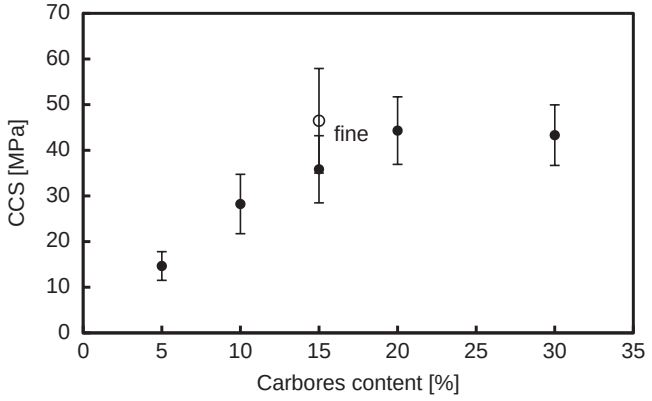

Fig. 7. Cold crushing strengths at different Carbores contents.

binder. The use of fine Carbores results in a CCS of 47 MPa. There is no significant further gain in strength in the use of 30 wt% binder.

3.3. Open porosity

The binder content has a significant influence on the porosity of the samples. Normally, with increasing binder content the fraction of air in the mixture decreases, thus the bulk density increases and the porosity decreases [12]. The reason is that a low binder content fills a smaller cavity volume, preventing the sliding of the grains during compaction and thus yields in a higher pore space. By increasing the binder content also a large amount of volatile components can escape and thus the porosity increases additionally [14]. Whereas pores resulting from pressing are conserved during coking, pores arising from pyrolysis are infiltrated immediately with liquid mesophases of Carbores® P [15].

The overall porosity depends on the pressing process. Uniaxial pressing achieves different compaction stages, reinforced by the strength of the granules and resulting in decline of porosities, cf. Fig. 8. Especially the fine

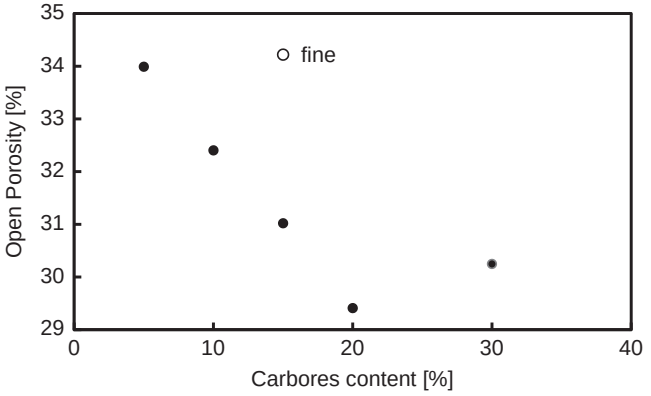

Fig. 8. Open Porosity as a function of the binder content.

Carbores leads to bad de-airing during pressing what causes an increase of the open porosity.

Regarding the evolution of the average pore radius, there is an increase from 68 nm to 199 nm from 5 to 30 wt% binder content, Table 4. Samples with 15 wt% fine Carbores offer higher pore sizes of about 127 nm caused by the inclusion of air during pressing, compared to samples with 15 wt% coarse Carbores with 81 nm. The 30 wt% Carbores content leads to a mean pore size of 199 nm, probably caused by a high amount of melting phase and cracking of the samples.

Considering the pore size distribution for the samples with different binder contents, from 5 wt% to 20 wt% Carbores® P the mean open pore size ranging from 100 to 500 nm is shifted to higher ratios, Fig. 9. The pore volume distribution is by this homogeneous as pore sizes < 100 nm and > 500 nm are marginal. Samples with 30 wt% Carbores ® P show a different distribution. Here, most of the pores have a wide radius distribution from 50 μm to 5 nm.

3.4. Bulk density

The density of the green and coked samples is subject to a maximum. Accordingly, the bulk density increases only as long as the binder replaces the air in the mixture. Due to the coarse nature of Carbores compared to alumina, replacing of air is insufficient. Therefore if the binder content is increased further, this only reinforces the layer between the alumina grains [14]. The resulting density is also highly influenced by the granules remaining in the structure. Due to the low specific weight of the binder of 1.35 g/cm^3, the increase of its fraction and the decrease of carbon black and graphite content with higher densities of approximately 1.7–1.9 g/cm^3 caused an additional decrease in bulk densities, Fig. 10.

3.5. Shrinkage

With higher Carbores content the shrinkage increases, Fig. 11, because more volatiles evaporate and a higher compaction of the microstructure through the curing of

Table 4
Average pore radius.

	AC 5	AC 10	AC 15	AC15 'fine'	AC 20	AC 30
Pore radius [nm]	68	67	81	127	82	199

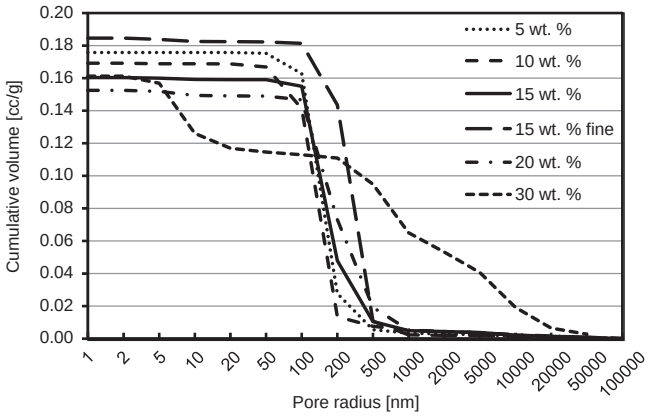

Fig. 9. Pore size distribution of the uniaxially pressed samples.

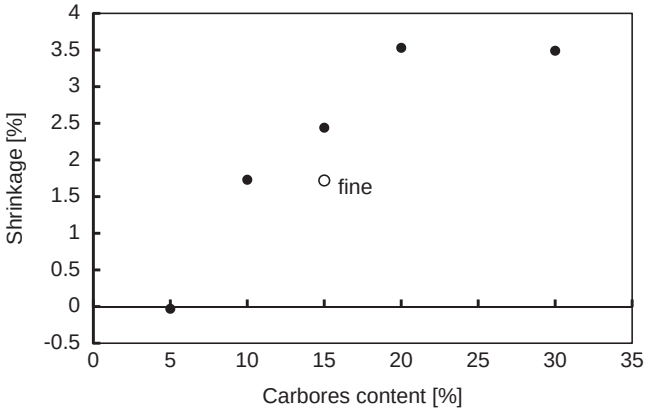

Fig. 11. Shrinkage as a function of the binder content.

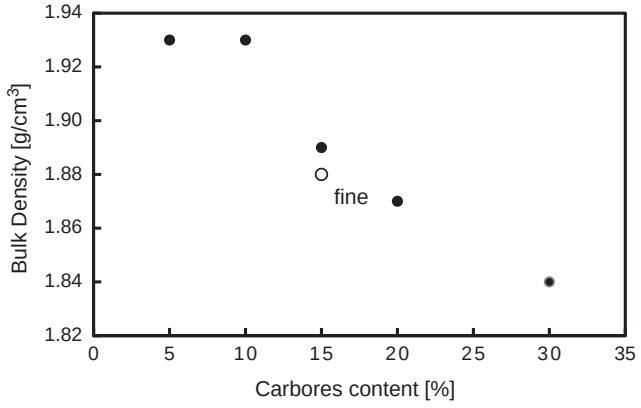

Fig. 10. Bulk density as a function of the binder content.

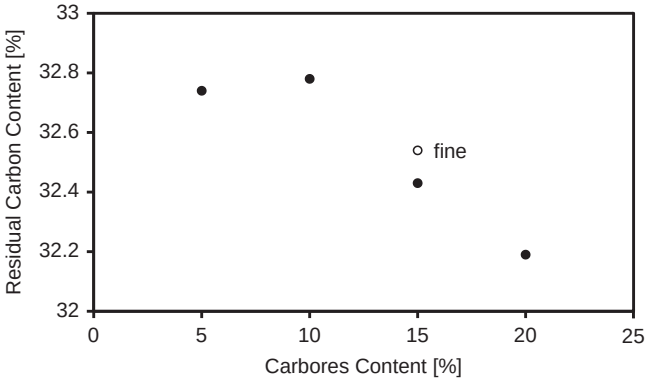

Fig. 12. Residual carbon content of uniaxially pressed samples.

pores can be achieved. Comparing the shrinkage rates to pure Al_2O_3, it has about 18% of shrinkage [13].

3.6. Residual carbon content

Considering the carbon content of the samples after coking, Fig. 12, its value is constant at 32–33 wt% for all contents of Carbores. Therefore, no variations in the mechanical strength due to different residual carbon contents can be expected.

However, also within the samples with the same binder content, the carbon content may yield varying properties. Measuring the carbon content of a sample with 20 wt% Carbores showed in the lateral region 31.3 wt% carbon and in the central area 32.8 wt% of carbon. A sample with 15 wt% Carbores showed 32.1 wt% in the lateral and 33.0 wt% carbon in the center. This slight deviation is compensated by averaging the CCS and CMOR tests of minimum 10 samples.

3.7. Scanning electron microscopy

The SEM images of the microstructure of samples containing 15 wt% coarse and fine binder, respectively, show a decisive difference, Fig. 13. The coarse binder grain is loosely distributed in the matrix and because of the grain size of the Carbores® P a constant binder film which completely surrounds the Al_2O_3 grains cannot be formed during pyrolysis. With 15 wt% fine Carbores® P it can be assumed that the grains can disperse more homogenous and the binder film is more distinctive. It is important to note that the function of the binder is not only to form a dense matrix but also to provide carbon for good high-temperature performance.

3.8. Fine and coarse grained carbon-bonded refractory materials with 30 wt% residual carbon

The production of carbon-bonded foam filters for clean steel production with the same composition as for the bulk material studied in this work was carried out by [6]. In contrast, for preparation of ceramic foam filters a viscous slurry was used, which was coated on a PU-foam block. After pyrolysis, this polyurethane skeleton was burned out, what leads to hollow filter struts. This leads to a higher shrinking rate, Table 5. However, the open porosity for samples with 20 wt% Carbores is approximately similar. The carbon content is for the bulk material somewhat higher.

Regarding the resulting microstructure, there is no apparent difference between the two fabrication routes, Fig. 14. The results confirm that the production of the bulk material with a similar composition according to [6] gives comparable microstructures.

In recent research there is a coarse grained Al_2O_3–C composition of Roungos [16] which consists of two types of alumina with a maximum grain size of 0.2 mm and 0.6 mm, compared to alumina in this work with a maximum size of 3 μm. It contains further coarse and fine graphite with a content of 29 wt% and grain sizes lower 40 μm and higher 70 μm. Therefore, the carbon content is the same as for the composition in this work. Novolak, a phenolic resin binder was used with a content of 6 wt%. Comparing this to the 5 wt% Carbores bonded bulk material of the present work, the open porosity is at 18%. That is the half of that of the bulk material with a porosity of 34%. Therefore the bulk density is at 2.39 g/cm^3, whereas it is at 1.96 g/cm^3 for the bulk material. Since the carbon content is approximately the same, the

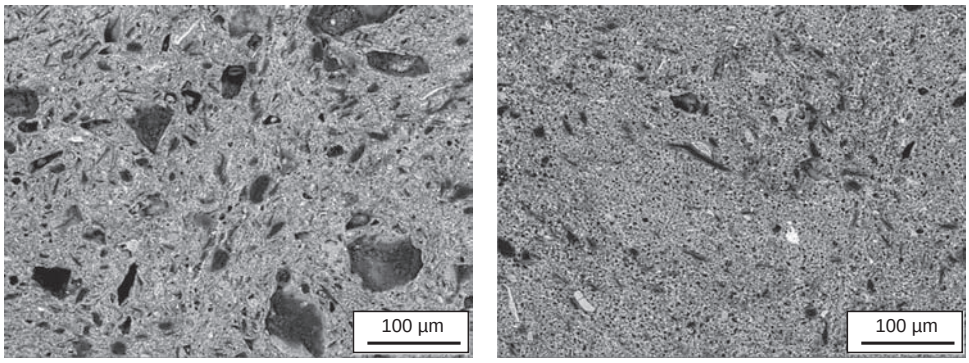

Fig. 13. SEM images of Al_2O_3–C containing 15 wt% coarse Carbores (left) and fine Carbores (right).

Table 5
Comparison of Al_2O_3–C bulk material with the ceramic foam filter of [6] and a coarse grained Al_2O_3–C composition of [16].

	Residual carbon [wt. %]	Open porosity [%]	Bulk density [g/cm^3]	Shrinkage [%]
20 **wt% Carbores**				
[6]	30.1	30.2		4.8
this work	32.2	29.4		3.5
5 **wt% Carbores**				
[16]	30.0	18.0	2.4	
this work	32.7	34.0	1.9	

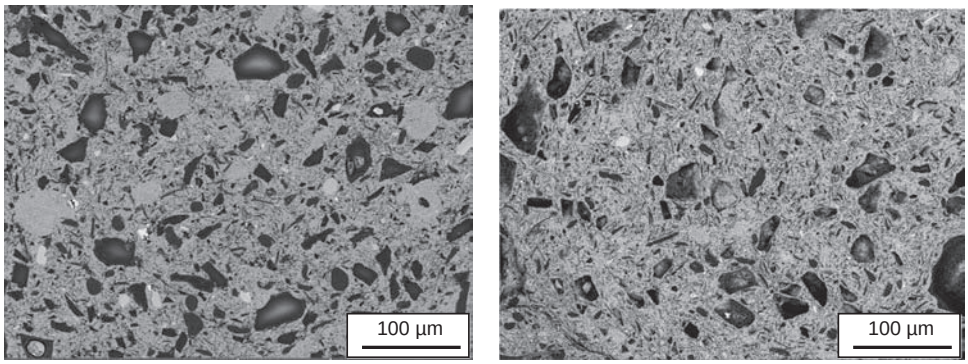

Fig. 14. SEM images of Al_2O_3–C with 20 wt% Carbores, left: foam filter [6] and right: bulk material.

coarse grained composition of Al_2O_3–C has a two times higher CMOR at a value of 16 MPa, [16].

This shows that a main improvement for achieving the matrix of Al_2O_3–C composition is a grain size of Carbores® P finer than for the alumina by supporting a binder film that is constantly distributed and increases bonding of the alumina grains and hence the mechanical properties.

4. Conclusions

A method for producing compact samples of carbon-bonded Al_2O_3–C which is developed as filter material for high quality steel melt filtration was studied. By isostatic shaping no crack free or even compact samples could be produced. In contrast, uniaxial pressing offers an adequate processing of bulk cylinders and sticks. However, residual granules in the material and edging effects resulting out of preparation could not be avoided and had an influence on the mechanical properties.

Beside this, CCS and CMOR values increase with increasing content of the coarse Carbores® P, whereas no significantly higher values can be achieved from 20 wt% to 30 wt% binder. The fine Carbores® P with 15 wt% gave an improved mechanical strength due to an enhanced homogeneity of the microstructure. The achieved CCS and CMOR are at the same level as for the coarse Carbores® P with 20 wt% and 30 wt%.

In terms of this contribution it was possible to produce fine grained bulk samples with a high amount of carbon and the same porosity level and pore size distribution as in already used slip casted filter materials of [6]. Based on the achieved bulk materials samples for investigating thermo-mechanical properties such as hot modulus of rupture, Young's modulus of elasticity and creep performance at elevated temperatures for modeling of filter materials can be obtained in the future.

Acknowledgments

The authors thank Dr. M. Hampel for professional input and practical realization, Dr. G. Schmidt and Dipl.-Ing. C. Segel for the scanning electron microscopy investigations, Mrs. C. Ludewig for the support in preparation, Mrs. U. Querner for the mercury pycnometry measurements, Mrs. J. Höhne for the strength tests and Mr. Rico Kaulfürst for the isostatic pressing. The studies were carried out with financial support from the Deutsche Forschungsgemeinschaft (DFG) within Collaborative Research Center SFB 920, Project C02.

References

[1] K. Raiber, D. Janke, Inclusion removal from Cr–Ni steel and Ni-base alloys using ceramic foam filters, Metall 49 (9) (1995) 574.
[2] C.G. Aneziris, F. Homola, D. Borzov, Material and process development of advanced refractories for innovative metal processing, Advanced Engineering Materials 6 (7) (2004) 563.
[3] V. Roungos, C.G. Aneziris, Prospects of developing self glazing Al_2O_3–C refractories for monobloc stopper applications, Refractory World Forum 3 (1) (2011) 94–98.
[4] K. Uemura, M. Takahashi, S. Koyama, M. Nitta, Filtration mechanism of non-metallic inclusions in steel by ceramic loop filter, ISIJ International 32 (1) (1992) 150.
[5] G. Routschka, H. Wuthnow (Eds.), Taschenbuch Feuerfeste Werkstoffe—Aufbau, Eigenschaften, Prüfung, 186, Vulkan-Verlag, Essen, 2007, p. 316.
[6] M. Emmel, C.G. Aneziris, Development of novel carbon bonded filter compositions for advanced steel melt filtration, Ceramics International 38 (6) (2012) 5165–5172.
[7] C.G. Aneziris, D. Borzov, J. Ulbricht, Magnesia-carbon bricks: a high-duty refractory material, Interceram Refractories Manual (2003) 22–27.
[8] W. Schatt, K.-P. Wieters, B. Kieback (Eds.), Springer Verlag, Berlin, Heidelberg, 2007 123.
[9] Boenigk, W., Pechstämmige Bindemittel für Feuerfestprodukte – Eigenschaften, Probleme und Perspektiven, 25. Feuerfest-Seminar (VDEh-Seminar 71/94), Bad Neuenahr, (1994).
[10] Lucke, R., Einfluss der am Einzelkorn einer keramischen Pressmasse bestimmten Parameter auf die Eigenschaften von Presslingen, Dissertation, Freiberg, (1989) pp. 61–64.
[11] W. Schulle, Anforderungen an und prüftechnische Beurteilung von Pressgranulaten, 73, Berichte der Deutschen Keramischen Gesellschaft, Berlin, 1996 81-86.
[12] P. Kleinschmidt, O. Vohler, M. Voll, E. Wege, H. Wirth, Kohlenstoffprodukte, in: H. Harnisch, R. Steiner, K. Winnaker (Eds.), Chemische Technologie, Carl Hanser Verlag, München, 1983, p. 287.
[13] Verband der Keramischen, Industrie e.V., Foliensatz Technische Keramik für Hochschulen, Fahner Druck GmbH, Lauf (2001) 23.
[14] Bach, U., Untersuchungen zur Bindung von kohlenstoffhaltigen Feuerfestmaterialien, Dissertation, Freiberg, 1991 p. 67.
[15] Y.W. Li, N. Li, C.G. Aneziris, M. Hampel, Physical and mechanical properties of environmental friendly carbon-bonded Al_2O_3–C—refractories for sliding gate applications, Berichte der Deutschen Keramischen Gesellschaft 84 (9) (2005) E55–E59.
[16] V. Roungos, C.G. Aneziris, Improved thermal shock performance of Al_2O_3–C refractories due to nanoscaled additives, Ceramics International 38 (2) (2012) 919–927.